

Persistent homology of unweighted complex networks via discrete Morse theory

Harish Kannan,¹ Emil Saucan,^{2,3} Indrava Roy,^{1,*} and Areejit Samal^{1,4,†}

¹*The Institute of Mathematical Sciences (IMSc),*

Homi Bhabha National Institute (HBNI), Chennai 600113 India

²*Department of Applied Mathematics, ORT Braude College, Karmiel 2161002 Israel*

³*Department of Electrical Engineering, Technion,*

Israel Institute of Technology, Haifa 3200003 Israel

⁴*Max Planck Institute for Mathematics in the Sciences, Leipzig 04103 Germany*

We present a new method based on discrete Morse theory to study topological properties of unweighted and undirected networks using persistent homology. Leveraging on the features of discrete Morse theory, our method produces a discrete Morse function that assigns weights to vertices, edges, triangles and higher-dimensional simplices in the clique complex of a graph in a concordant fashion. Importantly, our method not only captures the topology of the clique complex of such graphs via the concept of critical simplices, but also achieves close to the theoretical minimum number of critical simplices in several analyzed model and real networks. This leads to a reduced filtration scheme based on the subsequence of the corresponding critical weights. We have employed our new method to explore persistent homology of several unweighted model and real-world networks. We show that the persistence diagrams from our method can distinguish between the topology of different types of model and real networks. In summary, our method based on discrete Morse theory further increases the applicability of persistent homology to investigate global topology of complex networks.

INTRODUCTION

In recent years, the field of topological data analysis (TDA) has rapidly grown to provide a set of powerful tools to analyze various important features of data [1]. In this context, persistent homology has played a key role in bringing TDA to the fore of modern data analysis. It not only gives a way to visualize data efficiently, but also to extract relevant information from both structured and unstructured datasets. This crucial aspect has been used effectively in various applications from astrophysics (e.g., determination of inter-galactic filament structures) [2] to imaging analysis (e.g., feature detection in 3D gray-scale images) [3] to biology (e.g., detection of breast cancer type with high survival rates) [4]. Informally, the essence of the theory is its power to extract the *shape of data*, as well as infer high-order correlations between various parts of the data at hand which are missed by other classical techniques. The basic mathematical theory used in this subject is that of algebraic topology, and in particular the study of homology, developed by the French mathematician Henri Poincaré at the turn of the 20th century. The origins of persistent homology lie in the ideas of Morse theory [5], which gives a powerful tool to detect the topological features of a given space through the computation of homology using real-valued functions on the space. We refer the reader to the survey article [6] for further details.

On the other hand, the discretized version of Morse theory developed by Robin Forman [7, 8], gives a way to characterize the homology group of a simplicial complex in terms of a real-valued function with certain properties, known as a discrete Morse function. Examples of such simplicial complexes associated with discrete spaces are the Vietoris-Rips complex corresponding to a discrete metric space, or the clique complex of a graph. Forman showed [8] that given such a function, the so-called critical simplices completely determine the Euler characteristic of the space, which is a fundamental topological invariant.

The study of complex networks in the last few decades has also significantly raised our ability to understand various kinds of interactions arising in both natural and artificial realms [9–12]. Understanding how different parts of networks behave and influence each other is therefore an important problem [9–12]. However, for large networks, detecting higher order structures remains a difficult task [13]. While a graph representation captures binary relationships among vertices of a network, simplicial complexes also reflect higher-order relationships in a complex network [14–21]. In this context, persistent homology has been employed to explore the topological properties of complex networks [14–17, 19, 22]. In this work, we present a systematic method to study the persistent homology of unweighted and undirected graphs or networks. Previous work has investigated the persistent homology of weighted and undirected networks by creating a filtration of the clique complexes corresponding to threshold graphs obtained via decreasing

* Correspondence to: indrava@imsc.res.in

† Correspondence to: asamal@imsc.res.in

sequence of edge weights [16, 19]. However, the lack of edge weights in unweighted networks does not permit a filtration based on threshold graphs [16, 19]. Therefore, Horak *et al.* [15] study the persistent homology of unweighted and undirected networks based on a dimensional filtration scheme which adds at each filtration step p the p -skeleton of a simplicial complex. Another resolution would be to transform an unweighted network into a weighted network by assigning edge weights based on some network property, such as edge betweenness centrality [23, 24] or discrete edge curvature [25, 26], and then employing the filtration scheme based on threshold graphs [16, 19].

In the context of TDA, discrete Morse theory [7, 8] provides an efficient way of capturing the persistent homology of unweighted simple graphs. This is done by using the values given by the discrete Morse function to pass from an unweighted graph to a weighted simplicial complex (Figure 1). This transformation automatically produces a filtration that is needed for the computation of persistent homology, through the so-called level subcomplexes associated with critical simplices (See Theory section and Figure 2). Moreover, this filtration is consistent with the topology of the underlying space and reveals finer topological features than the dimensional filtration scheme used in [15]. The combination of these techniques have been used by Gunther *et al.* [3] with applications for image processing of 3D-grayscale images. However, to the best of our knowledge, this method has not been used for studying persistent homology in unweighted complex networks to date. Discrete Morse theory gives a theoretical lower bound on the number of critical simplices or filtration steps which can be attained by an optimal choice of the function on a simplicial complex. Interestingly, our method achieves close to the theoretical minimum number of critical simplices or filtration steps in several model and real networks analyzed here. Furthermore, our algorithm for computing the discrete Morse function is easy to implement for large complex networks.

Our results underline the potency of persistent homology to detect inherent topological features of networks which are not directly captured by homology alone. For instance, the p -Betti numbers of the clique complexes corresponding to small-world [9] and scale-free [10] networks with similar size and average degree, respectively, are of comparable magnitude and thus, homology reveals no deep insight into the differences between the topological features of these two model networks. On the other hand, our observations on the persistent homology of these two networks indicate a clear demarkation with respect to the evolution of topological features in the clique complexes corresponding to these model networks during the filtration process. This dissimilarity in the evolution of topological characteristics that resonates across dimensions and the average degree of the underlying network, indicates an inherent disparity in the persistent homology of small-world and scale-free graphs. The ability to capture inherent topological differences between two dissimilar networks thus motivates the application of our methods to study the persistent homology of real-world networks.

The remainder of the paper is organized as follows. We begin with a **Theory** section which gives a brief overview of concepts in homology, persistent homology and discrete Morse theory. We then proceed to describe the model networks and real-world networks that have been studied in this work in the **Network datasets** section. In the subsequent section on **Results and Discussion**, we present our algorithm to construct a discrete Morse function on a simplicial complex associated with a network and provide a rigorous proof of concept for the algorithm. We then follow up with two algorithms both of which illustrate key procedures that are essential to construct the filtration of a simplicial complex associated with the networks under study. In the same section, we present our results for model networks and real-world networks. The final section on **Conclusions** gives a summary and outlook of our findings.

THEORY

Graphs and Simplicial Complexes

Consider a finite simple graph $G(\mathcal{V}, \mathcal{E})$ having vertex set $\mathcal{V} = \{v_0, v_1, \dots, v_n\}$ and the edge set \mathcal{E} . Note that a simple graph does not contain self-loops or multi-edges [27]. Such a simple graph G can be viewed as a *clique* complex K [28]. A clique simplicial complex K is a collection of simplices where a p -dimensional simplex (or p -simplex) in K is a set of $p + 1$ vertices that form a complete subgraph. Note that the dimension p of simplices contained in K is restricted to the range 0 to the number of vertices $|\mathcal{V}|$ in the graph G . The dimension d of the clique complex K is given by the maximum dimension of its constituent simplices. A *face* γ of a p -simplex α is a subset of α such that γ is itself an l -simplex with dimension $0 \leq l < p$, and this relationship is denoted as $\gamma^l < \alpha^p$. In other words, vertices correspond to 0-simplices, edges to 1-simplices, and triangles to 2-simplices in the clique complex of a graph. Formally, the clique complex K corresponding to the simple graph G satisfies the following condition which defines an abstract simplicial complex, namely, K is a collection of non-empty finite sets or simplices such that if α is an element (simplex) of K then so is every non-empty subset of α . For additional details, the interested reader is referred to standard text in algebraic topology [29]. Figure 1 displays an example of the correspondence between a simple graph and its clique complex.

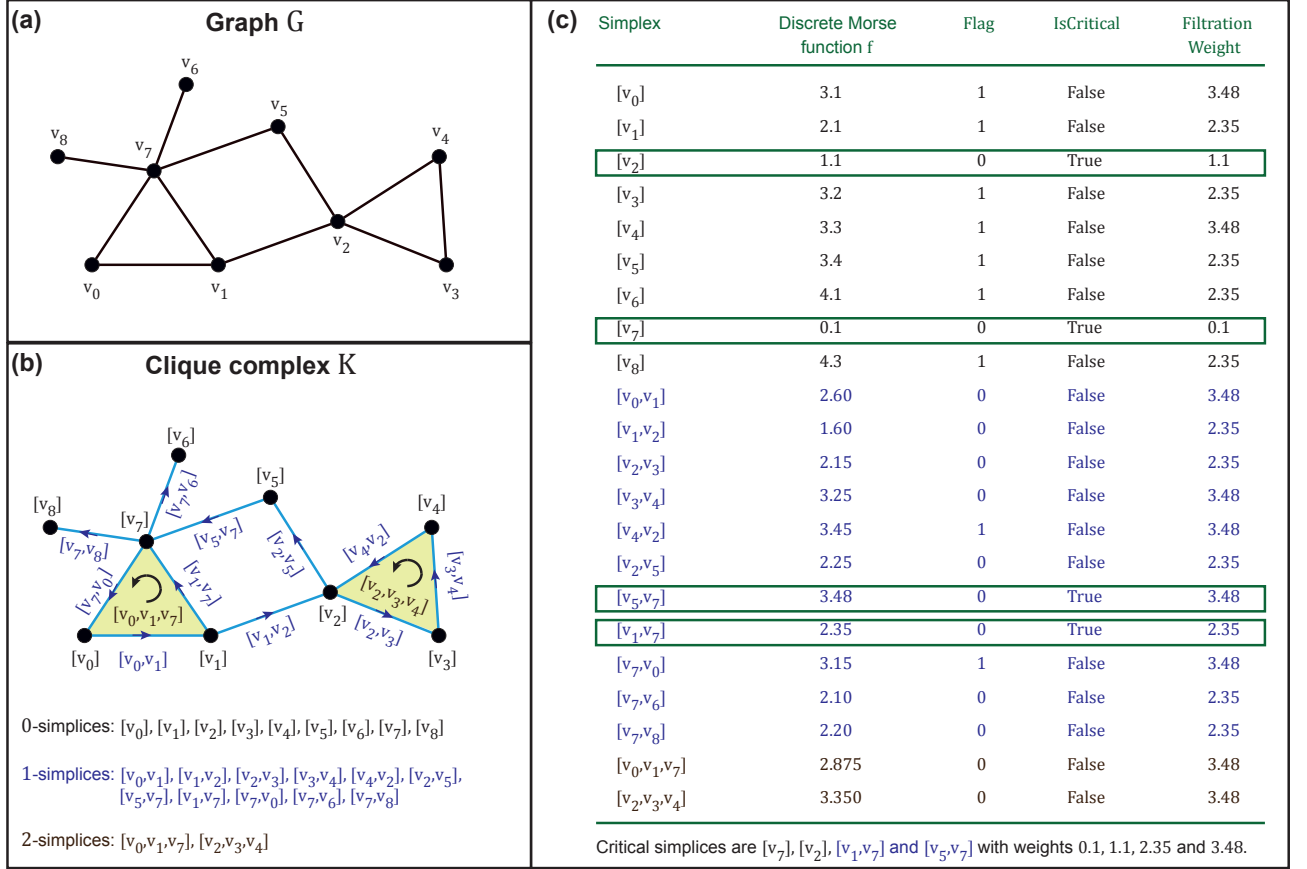


FIG. 1. An illustration of the construction of a discrete Morse function f on a clique complex K corresponding to an unweighted and undirected graph G using our algorithm. (a) A simple example of an unweighted and undirected graph G containing 9 vertices and 11 edges. (b) The clique simplicial complex K corresponding to the simple graph G shown in (a). The clique complex K consists of 8 vertices or 0-simplices, 11 edges or 1-simplices and 2 triangles or 2-simplices. The figure also displays the orientation of the 1- and 2-simplices using arrows. (c) Generation of a discrete Morse function f on the clique complex K shown in part (b) using our algorithm. The figure lists the state of the **Flag** variable in algorithm 1 and **IsCritical** variable in algorithm 2 for each simplex in K . In this example, the clique complex has 4 critical simplices and their corresponding critical weights are the filtration steps. The figure also lists the **FiltrationWeight** for each simplex in K obtained from algorithm 3.

Homology of a simplicial complex

The ordering of the vertex set $\{v_0, v_1, v_2, \dots, v_p\}$ of a p -simplex α determines its *orientation*. Moreover, two orderings of the vertex set of α are considered to be equivalent if and only if they differ by an even permutation. If the dimension of a p -simplex is greater than 1, then all possible orderings of its vertex set fall under two equivalence classes, with each class being assigned an *orientation* [29]. An exception is the 0-simplex with one vertex which has exactly one equivalence class and orientation. An oriented p -simplex α also specifies the orientation of its $p + 1$ vertices and is represented by $[v_0, v_1, v_2, \dots, v_p]$ [29]. In figure 1, the oriented 2-simplices $[v_2, v_3, v_4]$ and $[v_2, v_4, v_3]$ have opposite orientations, i.e., $[v_2, v_3, v_4] = -[v_2, v_4, v_3]$.

We next describe a mathematical group which provides the machinery to represent paths in a simplicial complex. The p -chain group C_p of a simplicial complex K is the Abelian group generated by the oriented p -simplices in K with coefficients in a field \mathbb{F} . Elements c of the p -chain group C_p are referred to as p -chains and have the form $c = \sum_i n_i \alpha_i$ where we use the same notation to represent both the oriented p -simplex and its corresponding generator in C_p and n_i are scalars from the field \mathbb{F} . Note that the identity element 0 in C_p is the unique p -chain for which all the coefficients n_i are zero in \mathbb{F} . Note also that if two p -simplices, α and β , have the same vertex set but opposite orientations, then the generators of C_p corresponding to the two simplices are inverse of each other (i.e., $\alpha = -\beta$). In figure 1, the cycle of length 4 formed by the edges or 1-simplices, $[v_1, v_2]$, $[v_2, v_5]$, $[v_5, v_7]$ and $[v_7, v_1]$, can be represented as an element of the 1-chain group which is $c = [v_1, v_2] + [v_2, v_5] + [v_5, v_7] - [v_7, v_1]$.

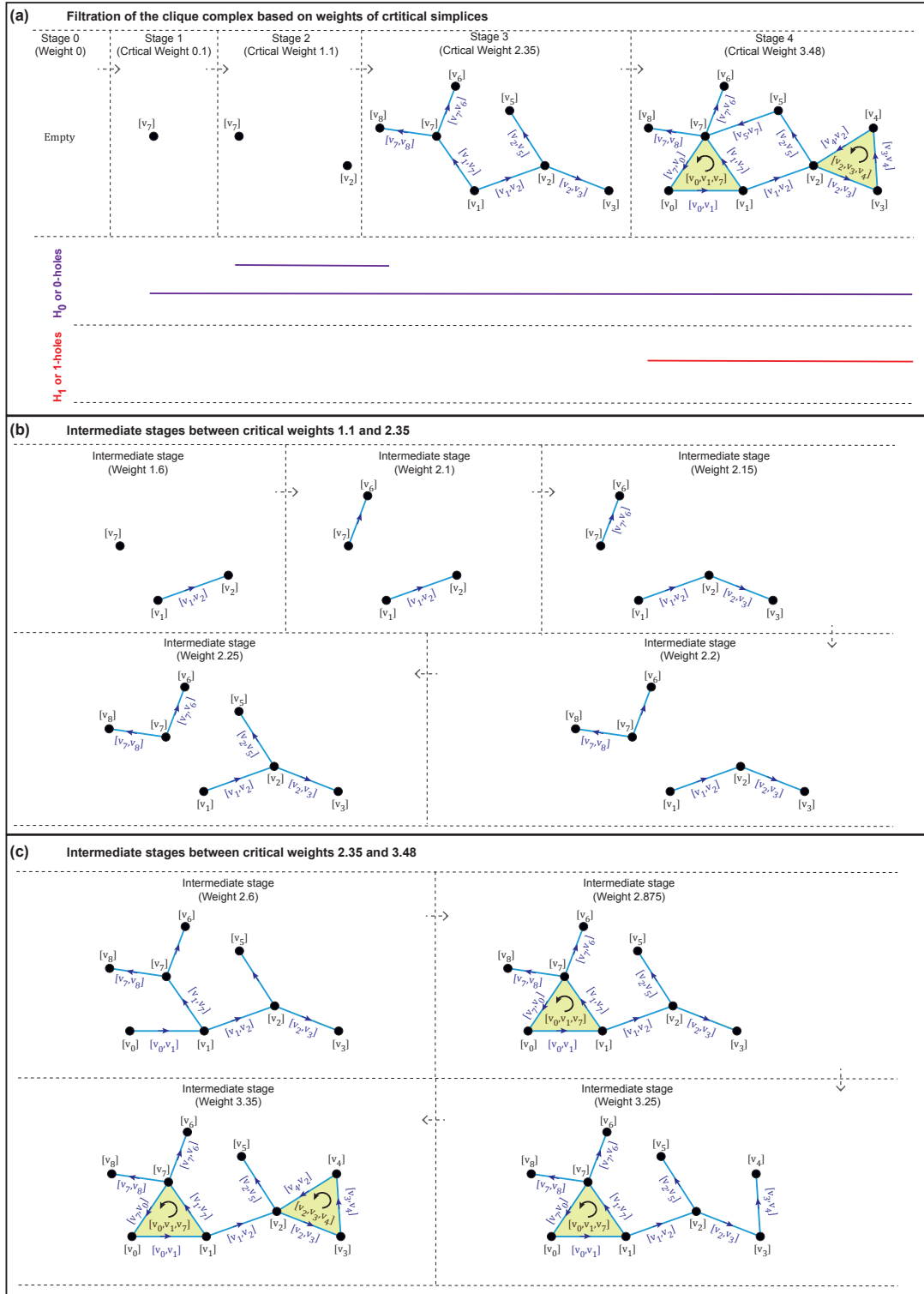


FIG. 2. Filtration based on the entire sequence of weights satisfying discrete Morse function is equivalent to filtration based only on the subsequence of critical weights in terms of persistent homology. (a) Filtration of the network shown in Figure 1 based on weights of the 4 critical simplices. There is a 0-hole (or connected component) that persists across the 4 stages of the filtration while another 0-hole is born at stage 2 on addition of critical vertex v_2 but dies at stage 3 on addition of the critical edge $[v_1, v_7]$. Moreover, a 1-hole is born at the stage 4 on addition of the critical edge $[v_5, v_7]$. (b) Five intermediate stages during the filtration between critical weights 1.1 (stage 2) and 2.35 (stage 3). (c) Four intermediate stages during the filtration between critical weights 2.35 (stage 3) and 3.48 (stage 4). It is seen that the homology of the clique complex remains unchanged during the intermediate stages of the filtration whereby the birth and death of holes occur only on addition of critical simplices.

The boundary operator ∂_p on the generator corresponding to an oriented p -simplex $\alpha = [v_0, v_1, \dots, v_p]$ is defined as follows [29]:

$$\partial_p(\alpha) = \sum_{i=0}^p (-1)^i [v_0, v_1, \dots, \hat{v}_i, \dots, v_p], \quad (1)$$

where \hat{v}_i refers to the absence of v_i in the $(p-1)$ -simplex. By linear extension, the boundary operator ∂_p on any element $c = \sum_i n_i \alpha_i$ of p -chain group C_p gives:

$$\partial_p(c) = \sum_i n_i \partial_p(\alpha_i) \quad (2)$$

Note that the boundary operator in the above equation maps a p -chain to a $(p-1)$ -chain. In figure 1, the boundary operator applied to the 1-chain $c = [v_0, v_1]$ representing an edge gives $v_1 - v_0$ while the boundary operator applied to the 1-chain $c = [v_1, v_2] + [v_2, v_5] + [v_5, v_7] + [v_7, v_1]$ representing a cycle of length 4 gives 0.

This motivates the definition of p -cycles Z_p and p -boundaries B_p . The p -cycles Z_p are the elements of the p -chain group C_p which are mapped to 0 by the boundary operator ∂_p , and thus:

$$Z_p = \ker(\partial_p) = \{c \in C_p \mid \partial_p(c) = 0\}. \quad (3)$$

The p -boundaries B_p is defined as follows:

$$B_p = \text{img}(\partial_{p+1}) = \{c \in C_p \mid \exists b \in C_{p+1}, \partial_{p+1}(b) = c\}. \quad (4)$$

Thus, p -boundaries B_p are the elements of the p -chain group C_p which also happen to be the boundary of an element in the $(p+1)$ -chain group C_{p+1} . Note that both Z_p and B_p are subgroups of the p -chain group C_p . It can be shown that the composition $\partial_{p-1} \circ \partial_p = 0$ which implies that B_p is a subgroup of Z_p [29]. Simply stated, it is true that the $(p-1)$ -boundary operator applied on a p -boundary gives 0. Hence, it follows that every p -boundary is a p -cycle but not necessarily vice versa.

The p -homology group is defined as [29]:

$$H_p = Z_p / B_p, \quad (5)$$

where Z_p/B_p is the quotient group [30] of Z_p over B_p . We informally refer to the elements of p -homology group H_p as p -holes. To provide an intuition for the definition of homology groups, a natural way to describe a p -hole would be to characterize it as a p -cycle which is not a p -boundary. In figure 1, the 1-cycle $c = [v_1, v_2] + [v_2, v_5] + [v_5, v_7] - [v_1, v_7]$ is a 1-hole as it is not a 1-boundary of any 2-chain while the 1-cycle $c = [v_2, v_3] + [v_3, v_4] - [v_2, v_4]$ is not a 1-hole as it is the 1-boundary of the 2-simplex $[v_2, v_3, v_4]$. Thus, the concept of quotient groups provide the mathematical machinery to characterize such p -holes in simplicial complexes.

The p -Betti number is defined as the dimension of the homology group H_p viewed as a vector space over field \mathbb{F} [29]. Informally, the p -Betti number β_p represents the number of p -holes of the simplicial complex. We remark that the Euler characteristic of the clique complex K with dimension d corresponding to a graph G is given by the alternating sum of Betti numbers [29], namely,

$$\chi(K) = \beta_0 - \beta_1 + \beta_2 - \dots + (-1)^d \beta_d. \quad (6)$$

In this work, we use the finite field $\mathbb{F} = \mathbb{Z}/2$, i.e., the field with two elements.

Persistent homology of a simplicial complex

A subset K^i of a simplicial complex K is called a subcomplex of K if K^i by itself is an abstract simplicial complex. Then a filtration of a simplicial complex K is defined as a nested sequence of subcomplexes K^i of K where:

$$\emptyset \subseteq K^0 \subseteq K^1 \subseteq \dots \subseteq K^q = K \quad (7)$$

Note that each subcomplex K^i has an associated index i in the filtration. Moreover, each subcomplex K^i in the filtration has corresponding p -chain complexes C_p^i , p -boundary operators ∂_p^i , p -boundaries B_p^i and p -cycles Z_p^i .

The j -persistent p -homology group of K^i denoted as $H_p^{i,j}$ is defined as:

$$H_p^{i,j} = Z_p^i / (B_p^{i+j} \cap Z_p^i). \quad (8)$$

In the above equation, B_p^{i+j} is the subgroup of C_p^{i+j} which constitutes the p -boundaries of the subcomplex K^{i+j} . The j -persistent p -Betti number of K^i denoted as $\beta_p^{i,j}$ is defined as:

$$\beta_p^{i,j} = \dim(H_p^{i,j}). \quad (9)$$

An intuitive explanation of the above definitions of the j -persistent p -homology group and the corresponding Betti number is as follows. A p -hole of the subcomplex K^i can potentially become the boundary of a $(p+1)$ -chain of a later subcomplex K^{i+j} with $j > 0$, and thus, no longer constitute a p -hole of K^{i+j} . The j -persistent p -Betti number of K^i represents the number of p -holes at the filtration index i that persist at the filtration index $j+i$. Therefore, each p -hole that appears across the filtration has a unique index that corresponds to its *birth* and *death*, and the persistence of such a p -hole can thus be characterized by its corresponding birth and death indices. Studying persistent homology allows us to quantify the longevity of such p -holes during filtration, and thus, measures the importance of these topological features which appear and disappear across the filtration.

Discrete Morse Theory

Recalling from the preceeding section, to study the persistent homology corresponding to the clique complex K of a simple graph G , the primary requirement is a filtration of K . Previous works [16, 19] which investigate the persistent homology of complex networks limit their study to weighted and undirected networks. The filtration of the clique complex K corresponding to a weighted graph G is constructed by forming a nested sequence of clique complexes which correspond to the threshold graphs of G obtained via decreasing sequence of the edge weights [16, 19]. In the context of unweighted and undirected networks, the absence of edge weights prohibits such a filtration scheme based on threshold graphs [16, 19]. A possible resolution would be to utilize network properties, such as edge betweenness centrality [23, 24] or discrete edge curvature [25, 26] to transform an unweighted network into a weighted network and then employing the filtration scheme based on threshold graphs. Taking an alternative route, Horak *et al.* [15] devised a filtration scheme based on the dimension of simplices [15] wherein all p -simplices of the clique complex K are added at the p^{th} filtration step.

In this work, we present a systematic method to study the persistent homology of unweighted and undirected networks by utilizing a refined filtration of the clique complex K . Our proposed scheme which is based on discrete Morse theory developed by Forman [7, 8] assigns weights to 0-simplices (vertices), 1-simplices (edges), 2-simplices (triangles) and higher-dimensional simplices appearing in the clique complex corresponding to an unweighted and undirected network. Assigning weights to higher-dimensional simplices captures important higher-order correlations in addition to edges or 1-simplices. Moreover, we leverage the following important features of the framework of discrete Morse theory in our new scheme. Firstly, the framework enables assignment of weights to p -simplices which are concordant with weights of $(p-1)$ -simplices. Secondly, it captures the topology of a simplicial complex via the concept of *critical* simplices described below. Thirdly, the framework provides a natural way to create a filtration scheme to study persistent homology based upon the weights of the aforementioned *critical* simplices as will be described below.

We next provide the fundamental definitions in discrete Morse theory [8]. We remark that a p -dimensional simplex α of a simplicial complex K is denoted by $\alpha^p \in K$ in the sequel. Given a function $f : K \rightarrow \mathbb{R}$, for each simplex $\alpha^p \in K$, two sets U_α^f and V_α^f are defined as follows:

$$U_\alpha^f = \{\beta^{p+1} \mid \alpha^p < \beta^{p+1} \text{ and } f(\beta) \leq f(\alpha)\} \quad (10)$$

$$V_\alpha^f = \{\gamma^{p-1} \mid \gamma^{p-1} < \alpha^p \text{ and } f(\alpha) \leq f(\gamma)\} \quad (11)$$

Simply stated, the set U_α^f contains any $(p+1)$ -simplex β^{p+1} of which α^p is a face and the function value on β is less than or equal to the function value on α . The set V_α^f contains any $(p-1)$ -simplex γ^{p-1} which is a face of α^p and the function value on α is less than or equal to the function value on γ . A function $f : K \rightarrow \mathbb{R}$ is a discrete Morse function [8] if and only if for each simplex $\alpha^p \in K$:

$$|U_\alpha^f| \leq 1 \text{ and } |V_\alpha^f| \leq 1. \quad (12)$$

Given a discrete Morse function f on the simplicial complex K , a simplex $\alpha^p \in K$ is critical [8] if and only if:

$$|U_\alpha^f| = 0 \text{ and } |V_\alpha^f| = 0. \quad (13)$$

We remark that once a discrete Morse function f on a simplicial complex K is fixed, the sets U_α^f and V_α^f are denoted by U_α and V_α , respectively, to simplify the notation. In the results section, we present our new scheme and algorithm 1 to assign a discrete Morse function f to a clique complex K of an unweighted graph G .

We next describe the filtration of the clique simplicial complex K based on the discrete Morse function f . Given a discrete Morse function f on a simplicial complex K and a real number r , a level subcomplex $K(r)$ is defined [8] as follows:

$$K(r) = \bigcup_{f(\beta) \leq r} \bigcup_{\alpha \leq \beta} \alpha \quad (14)$$

Simply stated, $K(r)$ contains all simplices β in K with the value of the discrete Morse function or assigned weight $f(\beta) \leq r$ along with any face α of β . Note that a face α of β is included in $K(r)$ even if the discrete Morse function or assigned weight to a face α is greater than r .

Let $\{f(\sigma)\}_{\sigma \in K}$ denote the entire set of values assigned to simplices in K using the discrete morse function f . Then, let $\{w_k\}_{k=0, \dots, n}$ denote the finite increasing sequence of the unique values in the set $\{f(\sigma)\}_{\sigma \in K}$ associated with the finite simplicial complex considered here. We now have a sequence of inclusions of level subcomplexes corresponding to this increasing sequence $\{w_k\}$ as follows:

$$\emptyset \subseteq K(w_0) \subseteq K(w_1) \subseteq \dots \subseteq K(w_{n-1}) \subseteq K(w_n) = K. \quad (15)$$

This nested sequence gives a filtration of the simplicial complex K which enables the study of persistent homology in the context of unweighted networks.

According to *Lemma 2.6 by Forman* [8], if there are no critical simplices α with $f(\alpha) \in (a, b]$, then $K(b)$ is *homotopy equivalent* to $K(a)$.

The implications of this Lemma are as follows. Let $\{f(\sigma_c)\}$ denote the set of values assigned to critical simplices σ_c in K by the discrete Morse function f and $\{w_{c_k}\}_{k=0, 1, \dots, m}$ denote the increasing sequence of the unique values in $\{f(\sigma_c)\}$. We refer to the function values $\{f(\sigma_c)\}$ assigned to the critical simplices σ_c in K as *critical weights*. Note that the set $\{f(\sigma_c)\}$ defined for critical simplices is a subset of $\{f(\sigma)\}$ defined for all simplices in K and the increasing sequence $\{w_{c_k}\}_{k=0, 1, \dots, m}$ is a subsequence of $\{w_k\}_{k=0, \dots, n}$ with $m \leq n$. The above definition implies that there are no critical simplices α with $f(\alpha) \in (w_{c_i}, w_{c_{i+1}})$. As homology is invariant under homotopy equivalence, Forman's Lemma 2.6 gives us that for any x and y belonging to the real number interval $(w_{c_i}, w_{c_{i+1}})$, the homology groups of $K(x)$ and $K(y)$ are isomorphic. Thus, in order to observe the changes in homology as the filtration proceeds, it suffices to study the persistent homology of a filtration which corresponds to the subsequence $\{w_{c_k}\}_{k=0, 1, \dots, m}$ of $\{w_k\}_{k=0, \dots, n}$, where $m \leq n$, and this results in a potential decrease in the required number of filtration steps. The new filtration sequence can be represented as:

$$\emptyset \subseteq K(w_{c_0}) \subseteq K(w_{c_1}) \subseteq \dots \subseteq K(w_{c_{m-1}}) \subseteq K(w_{c_m}) \subseteq K. \quad (16)$$

Note that each simplex α in the clique complex K is first introduced as part of certain level subcomplex $K(w_{c_i})$ in the above nested filtration sequence. Therefore, each simplex α in K can be associated with a unique weight w_{c_i} referred to as the filtration weight of α . In the results section, we present algorithm 2 and algorithm 3 which give the procedure to compute the filtration weights of simplices in the clique complex K of a graph G . Using an example network in figure 2, we also show that the persistent homology observed using the filtration based on the entire sequence of weights satisfying discrete Morse function is equivalent to that observed using the filtration based on the subsequence of critical weights.

Theorem 2.11 by Forman [8] can be stated as follows. Let m_p represent the number of critical p -simplices of dimension p in a simplicial complex K and β_p be the p -Betti number of K . Then, for each p , $m_p \geq \beta_p$.

In other words, the above theorem gives a lower bound of the number of p -critical simplices m_p for each dimension p as the p -Betti number β_p of K . In results section, we present our algorithm 1 to assign weights satisfying discrete Morse function to simplices in the clique complex K of a graph G . Our choice of the function in algorithm 1 to assign weights to simplices in the clique complex K tries to minimize the number of critical simplices (which has a lower bound given by Forman's Theorem 2.11 [8]), and thus, reduces the number of filtration steps required to compute the persistent homology without loss of information. In the results section, we will show that our algorithm achieves near-optimal number of critical weights in clique complexes corresponding to many model and real networks analyzed here.

Comparing Persistence diagrams

Given a filtration $\{K(w_{c_k})\}$ of the clique complex K of a graph G (See equation 16), each p -hole has a critical weight $w_{c_{birth}}$ which corresponds to its birth index and $w_{c_{death}}$ which corresponds to its death index, with $w_{c_{birth}} < w_{c_{death}}$. Persistence diagrams $\text{Dgm}(K)$ for a d -dimensional simplicial complex K is the collection of points in \mathbb{R}^2 whose first

and second coordinates, x and y , respectively, correspond to the birth weight and death weight of a p -hole of dimension $0 \leq p \leq d$ [31]. The persistence of a p -hole which has birth and death weights, $w_{c_{birth}}$ and $w_{c_{death}}$, respectively, is defined as $w_{c_{birth}} - w_{c_{death}}$. Thus, the persistence diagram for a clique complex K corresponding to a graph G is a compact representation of the persistent homology of a network.

Given two persistence diagrams X and Y (which may correspond to two different networks), the ∞ -Wasserstein distance between X and Y , also known as the *bottleneck distance*, is defined as follows [32]:

$$W_\infty(X, Y) = \inf_{\eta: X \rightarrow Y} \sup_{x \in X} \|x - \eta(x)\|_\infty^q. \quad (17)$$

Similarly, given two persistence diagrams X and Y , the q -Wasserstein distance between X and Y is defined as follows [32]:

$$W_q(X, Y) = \left[\inf_{\eta: X \rightarrow Y} \sum_{x \in X} \|x - \eta(x)\|_\infty^q \right]^{\frac{1}{q}}. \quad (18)$$

In the above equations, η ranges over all bijective maps from X to Y , and given $(a, b) \in \mathbb{R}^2$, $\|(a, b)\|_\infty = \max\{|a|, |b|\}$ is the L_∞ norm. Note that it is not generally true that two persistence diagrams X and Y have the same number of off-diagonal points, i.e., features with non-zero persistence, and we refer the readers to Kerber *et al.* [32] for details on circumventing this issue and further information regarding how the computation of the Wasserstein distance is reduced to a bipartite graph matching problem. In this work, we use Dionysus 2 package (<http://www.mrzv.org/software/dionysus2/>) to compute the Wasserstein distance between two persistence diagrams corresponding to two different model networks (See Results section). We remark that the bottleneck distance between two persistence diagrams which are subsets of the unit square is in the range 0 to 1.

NETWORK DATASETS

Model networks. We have investigated the following models of unweighted and undirected networks, namely, the Erdős-Rényi (ER) [33], the Watts-Strogatz (WS) [9], the Barabási-Albert (BA) [10] and the Hyperbolic Graph Generator (HGG) [34]. The ER model [33] is characterized by the property that the probability p of the existence of each possible edge between any two vertices among the n vertices in the graph G is constant. The existence of edges in the ER model are independent of each other, and thus, the model produces random graphs $G(n, p)$ with average vertex degree $p(n - 1)$. The WS model [9] produces small-world graphs as follows. The WS model starts with an initial regular graph with n vertices where each vertex is connected to its k nearest neighbours. Next, the endpoint of each edge in the initial regular graph of the WS model is randomly chosen for rewiring based on a fixed rewiring probability p and is rewired to another vertex in the graph which is chosen with uniform probability. The BA model [10] produces scale-free graphs which are characterized by a degree distribution that follows a power law decay. The BA model utilizes a preferential-attachment scheme to produce scale-free graphs. The BA model generates an initial graph of m_0 vertices, and then, at each successive iteration a new vertex is added with edges to m already existing vertices which are chosen with probability proportional to their degree at that particular iteration. The iterations in the BA model cease when the graph has attained the requisite number n of vertices. The HGG model [34, 35] produces a random graph of n vertices by initially fixing n vertices to n points on a hyperbolic disk. In the HGG model, the probability of existence of an edge between two vertices is proportional to the hyperbolic distance between the two points on the hyperbolic disk that correspond to these two vertices. By tuning the input parameter γ , the HGG model can produce either a hyperbolic or a spherical random graph [34, 35]. Specifically, the HGG model produces hyperbolic random graphs for $\gamma \in [2, \infty)$ whereas spherical random graphs for $\gamma = \infty$.

Real networks. We have also studied seven real-world networks which are represented as unweighted and undirected graphs. We have considered two biological networks, namely, the *Yeast protein interaction* network [36] with 1870 vertices and 2277 edges, and the *Human protein interaction* network [37] with 3133 vertices and 6726 edges. In both biological networks, each vertex represents a protein and an edge represents an interaction between the two proteins. We have considered two infrastructure networks including the *US Power Grid* network [38] and the *Euro road* network [39]. In the US Power Grid network, the 4941 vertices represent the generators, transformers and substations in the Western states of USA and the 6594 edges represent power links between them. The 1174 vertices of the Euro road network correspond to cities in Europe and the 1417 edges correspond to roads linking the cities. We have also studied the *Email* network [40] of the University of Rovira i Virgili with 1133 vertices representing users and 5451 edges, each representing the existence of at least one Email communication between the two users corresponding to the vertices anchoring the edge. We have also studied the *Route views* network [38] which has 6474 autonomous

Algorithm 1 Algorithm to construct a discrete Morse function on a d -dimensional simplicial complex K

```

1: function DISCRETEMORSEFUNCTION( $K, d, g$ )
2:   for  $p = 0, \dots, d$  do                                      $\triangleright$  Initialize Flag variable associated with each simplex in  $K$ 
3:     for each  $p$ -simplex  $\alpha \in K$  do
4:       Flag $[\alpha] = 0$ 
5:     end for
6:   end for

7:   for each 0-simplex  $\alpha \in K$  do                                $\triangleright$  Assign weights to 0-simplices in  $K$ 
8:      $f(\alpha) = g(\alpha)$ 
9:   end for

10:  for  $p = 1, \dots, d$  do
11:    for each  $p$ -simplex  $\alpha \in K$  do                                $\triangleright$  Assign weights to  $p$ -simplices in  $K$  with  $p \geq 1$ 
12:      Let Faces $[\ ]$  be an array of all  $(p-1)$ -dimensional faces of  $\alpha$ 
13:      Sort Faces $[\ ]$  such that  $f(\mathbf{Faces}[i]) \geq f(\mathbf{Faces}[i+1])$  for each  $i \in \{0, 1, \dots, p-1\}$ 
14:      Let  $\gamma_0 = \mathbf{Faces}[0]$ 
15:      Let  $\gamma_1 = \mathbf{Faces}[1]$ 
16:      if Flag $[\gamma_0] = 0$  and  $f(\gamma_0) > f(\gamma_1)$  then
17:         $f(\alpha) = (f(\gamma_0) + f(\gamma_1))/2$ 
18:        Flag $[\gamma_0] = 1$ 
19:      else
20:         $\epsilon = \text{random}(0, 0.5)$ 
21:         $f(\alpha) = f(\gamma_0) + \epsilon$ 
22:      end if
23:    end for
24:  end for

25:  return  $f$ 

26: end function

```

systems as vertices and 13895 edges representing communication between the systems that are represented as vertices. We have considered a social network, the *Hamsterster friendship* network [41], containing 1858 vertices which represent the users and 12534 edges which represent friendships between the users. Note that we omit self-loops while constructing the clique complex K corresponding to the undirected graph G of a real-world network.

RESULTS AND DISCUSSION

Algorithm to construct discrete Morse function on a simplicial complex

From an unweighted and undirected graph $G(\mathcal{V}, \mathcal{E})$ with vertex set \mathcal{V} and edge set \mathcal{E} , it is straightforward to construct a clique simplicial complex K with dimension d (See Theory section). Figure 1 shows the construction of a clique complex starting from an example network. Given a simplicial complex K , its dimension d and a non-negative real-valued function g on the 0-simplices of K , the algorithm 1 assigns weights to any simplex in K , producing a discrete Morse function f defined in equation 12. In the pseudocode of the algorithm 1, lines 2-6 initialize a variable **Flag** $[\alpha]$ for every simplex α in clique complex K with the value 0. We remark that the variable **Flag** $[\alpha]$ associated with a simplex α in K serves as a counter for the size of the set U_α defined in equation 10. Lines 7-9 assign weights to every 0-simplex in K based on the input non-negative function g . Lines 10-24 assign weights to 1- or higher-dimensional simplices in K in a manner which is consistent with the definition in equation 12 of a discrete Morse function. In summary, the algorithm 1 outputs a discrete Morse function f on K and we now present a rigorous proof for the following theorem using results from Lemmas 1 to 5 described later.

Theorem. *Algorithm 1 produces a discrete Morse function f on any simplicial complex K of finite dimension d .*

Proof. Let K denote a simplicial complex of dimension d . Recall that for the function f on K which is constructed by algorithm 1, for each simplex $\alpha^p \in K$, the two sets U_α and V_α were defined in equations 10 and 11 as follows:

$$\begin{aligned} U_\alpha &= \{\beta^{p+1} \mid \alpha^p < \beta^{p+1} \text{ and } f(\beta) \leq f(\alpha)\} \\ V_\alpha &= \{\gamma^{p-1} \mid \gamma^{p-1} < \alpha^p \text{ and } f(\alpha) \leq f(\gamma)\} \end{aligned}$$

To prove that f is a discrete Morse function we need to show that for each simplex $\alpha \in K$, both $|V_\alpha| \leq 1$ and $|U_\alpha| \leq 1$ (See equation 12).

Firstly, we show that for each simplex $\alpha \in K$, $|V_\alpha| \leq 1$. Consider a 0-simplex $\alpha \in K$. Since, the dimension of a simplex cannot be less than 0, for each 0-simplex $\alpha \in K$ the corresponding set V_α is empty. In other words, for each 0-simplex $\alpha \in K$, we have that $|V_\alpha| = 0$. Also, for each p -simplex $\alpha^p \in K$ such that $1 \leq p \leq d$, Lemma 5 below shows that $|V_\alpha| \leq 1$. Thus, for every simplex $\alpha \in K$, we have shown that $|V_\alpha| \leq 1$.

Secondly, we show that for each simplex $\alpha \in K$, $|U_\alpha| \leq 1$. For each p -simplex $\alpha^p \in K$ such that $0 \leq p \leq (d-1)$, we prove in Lemma 4 below that $|U_\alpha| \leq 1$. Now consider a d -simplex $\alpha^d \in K$. Since, by assumption K is a d -dimensional simplicial complex, there are no $(d+1)$ -simplices in K , and thus, the set U_α for each d -simplex $\alpha^d \in K$ is empty. In other words, for each d -simplex $\alpha^d \in K$, we have that $|U_\alpha| = 0$. Thus, for every simplex $\alpha \in K$ we have shown that $|U_\alpha| \leq 1$.

In summary, we have shown that for each simplex $\alpha \in K$, $|V_\alpha| \leq 1$ and $|U_\alpha| \leq 1$. Thus, f satisfies the definition of a discrete Morse function on the simplicial complex K (See equation 12). \square

We next prove the Lemmas used in the proof of the theorem above. This is done in the following sequence of Lemmas 1 to 5. We assume that K is a d -dimensional simplicial complex and f is the output function on K obtained from algorithm 1. We *remark* that a p -dimensional simplex α of a simplicial complex K is denoted by $\alpha^p \in K$. Also, if p -simplex α is a face of a $(p+1)$ -simplex β then this is represented as $\alpha^p < \beta^{p+1}$ in the sequel.

Lemma 1. *For each p where $0 \leq p \leq (d-1)$, if $\alpha^p \in K$ and $\beta^{p+1} \in K$ such that $\alpha^p < \beta^{p+1}$, then, $f(\alpha) \neq f(\beta)$.*

Proof. Let $\gamma_0, \gamma_1, \dots, \gamma_{p+1}$ denote the p -dimensional faces of β^{p+1} such that $f(\gamma_0) \geq f(\gamma_1) \geq \dots \geq f(\gamma_{p+1})$. Note that α^p is one such γ_i since by assumption α^p is a p -dimensional face of β^{p+1} . Based on lines 11-23 in algorithm 1, we have that:

$$f(\beta) = \begin{cases} (f(\gamma_0) + f(\gamma_1))/2 & \text{if } \mathbf{Flag}[\gamma_0] = 0 \text{ and } f(\gamma_0) > f(\gamma_1) & \text{(Case A)} \\ f(\gamma_0) + \epsilon & \text{otherwise} & \text{(Case B)} \end{cases} \quad (19)$$

where $\epsilon > 0$.

Case A implies $f(\gamma_0) > f(\beta) > f(\gamma_1) \geq f(\gamma_2) \dots \geq f(\gamma_p) \geq f(\gamma_{p+1})$.

Case B implies $f(\beta) > f(\gamma_0) \geq f(\gamma_1) \geq f(\gamma_2) \dots \geq f(\gamma_p) \geq f(\gamma_{p+1})$.

Thus, for both cases we have that $f(\beta) \neq f(\gamma_i)$ for each $i \in \{0, 1, 2, \dots, (p+1)\}$. Since α^p is one such γ_i for some $i \in \{0, 1, 2, \dots, (p+1)\}$, we have $f(\alpha) \neq f(\beta)$. \square

Lemma 2. *For each p where $0 \leq p \leq (d-1)$, if $\alpha^p \in K$ and $\beta^{p+1} \in K$ such that $\alpha^p < \beta^{p+1}$, then $f(\alpha) > f(\beta)$ if and only if $\mathbf{Flag}[\alpha]$ changes value from 0 to 1 while assigning function value for β .*

Proof. Given $\alpha^p \in K$ and $\beta^{p+1} \in K$ such that $\alpha^p < \beta^{p+1}$, we first assume $f(\alpha) > f(\beta)$. Let $\gamma_0, \gamma_1, \dots, \gamma_{p+1}$ denote the p -dimensional faces of β^{p+1} such that $f(\gamma_0) \geq f(\gamma_1) \geq \dots \geq f(\gamma_{p+1})$. Then, the value $f(\beta)$ is given by equation 19.

Case A in equation 19 implies $f(\gamma_0) > f(\beta) > f(\gamma_1) \geq f(\gamma_2) \dots \geq f(\gamma_p) \geq f(\gamma_{p+1})$.

Case B in equation 19 implies $f(\beta) > f(\gamma_0) \geq f(\gamma_1) \geq f(\gamma_2) \dots \geq f(\gamma_p) \geq f(\gamma_{p+1})$.

Since by assumption, α^p is a face of β^{p+1} and $f(\alpha) > f(\beta)$, Case A is applicable, and we have γ_0 equals α^p . Thus, based on line 18 in algorithm 1, while assigning the function value on β^{p+1} , $\mathbf{Flag}[\alpha]$ changes value from 0 to 1.

Now, given $\alpha^p \in K$ and $\beta^{p+1} \in K$ such that $\alpha^p < \beta^{p+1}$, we assume that $\mathbf{Flag}[\alpha]$ changes value from 0 to 1 while assigning function value for β^{p+1} . Let $\gamma_0, \gamma_1, \dots, \gamma_{p+1}$ denote the p -dimensional faces of β^{p+1} such that $f(\gamma_0) \geq f(\gamma_1) \geq \dots \geq f(\gamma_{p+1})$. Based on lines 11-23 in algorithm 1, $\mathbf{Flag}[\alpha]$ changes value from 0 to 1 while assigning

function value for β^{p+1} implies that γ_0 equals α^p . Thus, we have that $f(\alpha) > f(\beta) = (f(\alpha) + f(\gamma_1))/2$. \square

Lemma 3. *Let α be a simplex of K . Then, the number of times $\mathbf{Flag}[\alpha]$ changes value from 0 to 1 is ≤ 1 .*

Proof. $\mathbf{Flag}[\alpha]$ is initially set to 0 in algorithm 1. In algorithm 1, if $\mathbf{Flag}[\alpha]$ transitions to 1, its value never changes. In other words, there is no procedure in our algorithm 1 which changes the \mathbf{Flag} of a simplex from 1 to 0. Thus, either $\mathbf{Flag}[\alpha]$ remains 0 throughout or changes value from 0 to 1 exactly once in algorithm 1. \square

Lemma 4. *For each p where $0 \leq p \leq (d-1)$, if $\alpha^p \in K$, then $|U_\alpha| \leq 1$.*

Proof. From Lemma 2, we have that for each $\alpha^p \in K$, the number of $(p+1)$ -simplices β^{p+1} such that $\alpha^p < \beta^{p+1}$ and $f(\beta) < f(\alpha)$ is equal to the number of times $\mathbf{Flag}[\alpha]$ changes value from 0 to 1. Applying Lemma 3, we get that for each $\alpha^p \in K$,

$$\#\{\beta^{p+1} \mid \alpha^p < \beta^{p+1} \text{ and } f(\beta) < f(\alpha)\} \leq 1.$$

Furthermore, Lemma 1 tells us that,

$$\#\{\beta^{p+1} \mid \alpha^p < \beta^{p+1} \text{ and } f(\beta) < f(\alpha)\} = \#\{\beta^{p+1} \mid \alpha^p < \beta^{p+1} \text{ and } f(\beta) \leq f(\alpha)\}$$

Thus, we have that for each $\alpha^p \in K$, $|U_\alpha| = \#\{\beta^{p+1} \mid \alpha^p < \beta^{p+1} \text{ and } f(\beta) \leq f(\alpha)\} \leq 1$. \square

Lemma 5. *For each p where $1 \leq p \leq d$, if $\alpha^p \in K$, then $|V_\alpha| \leq 1$.*

Proof. Let $\gamma_0, \gamma_1, \dots, \gamma_p$ denote the $(p-1)$ -dimensional faces of $\alpha^p \in K$ such that $f(\gamma_0) \geq f(\gamma_1) \geq \dots \geq f(\gamma_p)$. Based on lines 11-23 in algorithm 1, we have that:

$$f(\alpha) = \begin{cases} (f(\gamma_0) + f(\gamma_1))/2 & \text{if } \mathbf{Flag}[\gamma_0] = 0 \text{ and } f(\gamma_0) > f(\gamma_1) & \text{(Case A)} \\ f(\gamma_0) + \epsilon & \text{otherwise} & \text{(Case B)} \end{cases}$$

where $\epsilon > 0$.

Case A implies $f(\gamma_0) > f(\alpha) > f(\gamma_1) \geq f(\gamma_2) \dots \geq f(\gamma_{p-1}) \geq f(\gamma_p)$, and thus, $|V_\alpha| = 1$.

Case B implies $f(\alpha) > f(\gamma_0) \geq f(\gamma_1) \geq f(\gamma_2) \dots \geq f(\gamma_{p-1}) \geq f(\gamma_p)$, and thus, $|V_\alpha| = 0$.

Hence, for each $\alpha^p \in K$ with $1 \leq p \leq d$, we have that $|V_\alpha| \leq 1$. \square

Filtration of the clique complex based on weights of critical simplices

Given a simplicial complex K , its dimension d and a discrete Morse function f on K , the algorithm 2 determines the weights of critical simplices in K (See equation 13). In the pseudocode of the algorithm 2, lines 2-6 initialize a variable $\mathbf{IsCritical}[\alpha]$ associated to every simplex α in clique complex K to be True. Lines 7-20 determine the critical simplices in K by checking for the condition in equation 13 which defines a critical simplex. Lines 21-31 determine the weights of critical simplices or critical weights in K . Finally, the algorithm 2 outputs an array $w_c[]$ which contains an increasing sequence of critical weights in K . Subsequently, this increasing sequence of critical weights will be used for the filtration of the clique complex K .

Given an unweighted and undirected graph G , we restrict the construction of clique complex K by including simplices up to a maximum dimension d . Then, the algorithm 3 creates the filtration of clique complex K based on weights of critical simplices as described in the Theory section. In the pseudocode of the algorithm 3, lines 2-6 assigns a non-negative function g to 0-simplices in clique complex K . Line 7 calls the algorithm 1 for the assignment of weights satisfying discrete Morse function to every simplex in K . Line 8 calls the algorithm 2 to obtain an increasing sequence of unique weights corresponding to critical simplices in K . Lines 9-11 initialize a variable $\mathbf{IsAdded}[\alpha]$ associated to every simplex α in K which tracks whether the simplex α has been added to the filtration or not. Lines 12-25 compute the filtration weight of each simplex α in K as described in the Theory section.

Rationale for the choice of function on vertices

In order to construct a discrete Morse function f on clique complex K corresponding to a graph G using our algorithm 1, a real-valued function g has to be fixed on the 0-simplices of K (See lines 7-9 in algorithm 1). Let deg_{max}

Algorithm 2 Algorithm to compute the weights of critical simplices in K

```

1: function GETCRITICALWEIGHTS( $K, d, f$ )
2:   for  $p = 0, \dots, d$  do                                     ▷ Initialize IsCritical variable associated with each simplex in  $K$ 
3:     for each  $p$ -simplex  $\alpha \in K$  do
4:       IsCritical[ $\alpha$ ] = True
5:     end for
6:   end for
7:   for  $p = 1, \dots, d$  do                                     ▷ Determine the critical simplices in  $K$ 
8:     for each  $p$ -simplex  $\alpha \in K$  do
9:       Let Faces[ ] be an array of all  $(p-1)$ -dimensional faces of  $\alpha$ 
10:      Sort Faces[ ] such that  $f(\text{Faces}[i]) \geq f(\text{Faces}[i+1])$  for each  $i \in \{0, 1, \dots, p-1\}$ 
11:      Let  $\gamma_0 = \text{Faces}[0]$ 
12:      Let  $\gamma_1 = \text{Faces}[1]$ 
13:      if  $f(\gamma_0) \geq f(\alpha)$  then
14:        IsCritical[ $\alpha$ ] = False
15:        if IsCritical[ $\gamma_0$ ] = True then
16:          IsCritical[ $\gamma_0$ ] = False
17:        end if
18:      end if
19:    end for
20:  end for
21:  Initialize  $i = 0$ 
22:  Declare empty array  $w_c$ [ ]
23:  for  $p = 0, \dots, d$  do                                     ▷ Determine the weights of critical simplices in  $K$ 
24:    for each  $p$ -simplex  $\alpha \in K$  do
25:      if IsCritical[ $\alpha$ ] = True then
26:         $w_c[i] = f(\alpha)$ 
27:         $i = i + 1$ 
28:      end if
29:    end for
30:  end for
31:  Sort array  $w_c$ [ ] in increasing order and remove duplicates
32:  return  $w_c$ [ ]
33: end function

```

denote the maximum degree of a vertex in the graph $G(\mathcal{V}, \mathcal{E})$. Our choice for the function value on the vertices or 0-simplices, $g : \mathcal{V} \rightarrow \mathbb{R}$, is as follows:

$$g(v) = \deg_{\max} - \text{degree}(v) + \epsilon \quad (20)$$

where $\text{degree}(v)$ is the degree of the vertex $v \in G$ and ϵ is a random number (noise) chosen uniformly in the range $(0, 0.5)$. See lines 2-6 in algorithm 3 and lines 7-9 in algorithm 1.

In the Theory section, we had highlighted the Theorem 2.11 by Forman [8] which gives a lower bound on the number of critical p -simplices, m_p , in a simplicial complex K as the p -Betti number β_p . The choice of the real-valued function g in algorithm 1 plays a key role in determining if the number m_p of critical p -simplices in K is close to the theoretical minimum β_p stated above. In the Theory section, we have shown that the number of critical simplices determines the effective number of filtration weights to study the persistent homology of a clique complex (See equation 16). This motivated our choice for the real-valued function (equation 20) which determines the weights of 0-simplices, and the rationale for this choice is as follows.

Ignoring the noise term ϵ in equation 20, the reader can discern our intuition for choosing the function $g(v) = \deg_{\max} - \text{degree}(v)$ for any vertex v in G with the following example. Consider the simple example of the clique complex K corresponding to a graph G in figure 1. Here, we would like to obtain a discrete Morse function f on K such that the number of critical simplices is close to the theoretical minimum. This requirement applies to simplices of any dimension in K , and in the context of this example, we would like the number of critical 1-simplices (edges) to

Algorithm 3 Algorithm to create the filtration of a clique complex K

```

1: Create clique complex  $K$  of graph  $G$  by restricting to a maximum dimension  $d$ 

2:  $deg_{max}$  = Maximum degree of a vertex in graph  $G$ 
3: for each 0-simplex  $\alpha \in K$  do                                     ▷ Assign non-negative function  $g$  to 0-simplices in  $K$ 
4:    $\epsilon = \text{random}(0, 0.5)$ 
5:    $g[\alpha] = deg_{max} - \text{degree}(\alpha) + \epsilon$ 
6: end for

7:  $f = \text{DISCETEMORSEFUNCTION}(K, d, g)$                                ▷ Call Algorithm 1
8:  $w_c[\ ] = \text{GETCRITICALWEIGHTS}(K, d, f)$                              ▷ Call Algorithm 2

9: for each simplex  $\alpha \in K$  do                                       ▷ Initialize IsAdded variable associated with each simplex in  $K$ 
10:   IsAdded $[\alpha] = \text{False}$ 
11: end for

12: for  $i = 0, \dots, \text{len}(w_c[\ ]) - 1$  do                               ▷ Calculate Filtration weight for each simplex in  $K$ 
13:   for each simplex  $\alpha \in K$  do
14:     if  $f(\alpha) \leq w_c[i]$  AND IsAdded $[\alpha] = \text{False}$  then
15:       FiltrationWeight $[\alpha] = w_c[i]$ 
16:       IsAdded $[\alpha] = \text{True}$ 
17:       for each face  $\gamma < \alpha$  do
18:         if IsAdded $[\gamma] = \text{False}$  then
19:           FiltrationWeight $[\gamma] = w_c[i]$ 
20:           IsAdded $[\gamma] = \text{True}$ 
21:         end if
22:       end for
23:     end if
24:   end for
25: end for

```

be as close as possible to the 1-Betti number β_1 of K . Note that $\beta_1 = 1$ for the example clique complex K in figure 1.

Let us now examine lines 11-23 in algorithm 1. Consider any edge $e_{vw} = [v, w]$ such that $g(v) > g(w)$. While assigning the function value to the edge e_{vw} in algorithm 1, the edge e_{vw} and the vertex v are guaranteed to be not critical provided that the *if condition* in the line 16 is satisfied. This is a consequence of the definition of a critical simplex (See equation 13). Thus, we would like to force this *if condition* to be True for as many edges as possible. Moreover, once the function value of the 1-simplex e_{vw} is set, we set the variable **Flag** $[v]$ to 1 in line 18, and this subsequently forces the *if condition* in the line 16 to fail for all other edges $e_{vz} = [v, z]$ in the graph that contain v and have function value $g(v) > g(z)$.

Let us now examine the edge $e_{78} = [v_7, v_8]$ in figure 1 which is anchored by vertices v_7 and v_8 with degree 5 and 1, respectively. As the degree of a vertex gives the number of edges that contain the vertex, v_7 is part of 4 other edges while v_8 is part of only the edge e_{78} . Suppose e_{78} is the first edge chosen for the function assignment in line 11 of algorithm 1 and both **Flag** $[v_7]$ and **Flag** $[v_8]$ for the anchoring vertices are 0. As v_7 is part of 4 other edges while v_8 is part of only e_{78} , we would then prefer that the *if condition* in the line 16 is satisfied for e_{78} , and furthermore, **Flag** $[v_8]$ is set to 1 instead of **Flag** $[v_7]$, in other words, we need the function value $g(v_8) > g(v_7)$. We emphasize that this choice of v_8 over v_7 prevents the forced failure (described in the previous paragraph) of the *if condition* for the 4 other edges that contain v_7 .

The above example suggests a need for a function g on the vertices that has an inverse relationship with the degree of the vertices. For instance, if the function on vertices was chosen to be $g(v) = \text{degree}(v)$, then every edge except e_{78} containing v_7 would become critical, since v_7 has the maximum degree in the example network. Hence, our choice $g(v) = deg_{max} - \text{degree}(v)$ provides a simple and effective solution for the above requirement.

We now provide a rationale for the addition of a random noise ϵ in equation 20. As reasoned above, we would like to force the *if condition* in the line 16 of algorithm 1 to be True for as many edges as possible. Consider any edge $e_{vw} = [v, w]$ such that $g(v) = g(w)$. Then, irrespective of the state of **Flag** $[v]$ and **Flag** $[w]$, the *if condition* fails. Hence, we would like $g(v) \neq g(w)$ while also retaining the inverse relationship of the function with the degree. Adding a small random noise ϵ in the range $(0, 0.5)$ provides a simple resolution (See equation 20). We remark that the above

argument can be generalized to higher-dimensional simplices, and thus, provides the intuition for the addition of noise ϵ in line 21 of algorithm 1.

We remind the readers that our initial motivation was not to develop a scheme to construct the optimal discrete Morse function on a clique complex corresponding to a graph. Rather, our main goal is to develop a systematic filtration scheme to study persistent homology in unweighted and undirected networks. In fact, constructing an optimal discrete Morse function in the general case has been shown to be MAX-SNP Hard [42]. The primary utility of our scheme is to create a filtration by assigning weights to simplices in the clique complex K of a graph G . However, we next report our empirical results from an exploration of model and real-world networks which underscore the following. Although our scheme is not optimal in the sense of minimizing the number of critical simplices, in practice, it achieves near-optimal results in several model and real-world networks (Table I). Hence, our scheme based on discrete Morse theory reduces the number of filtration steps and increases the applicability of persistent homology to study complex networks.

TABLE I. The table lists the number of p -simplices (n_p), the number of critical p -simplices (m_p) and the p -Betti number β_p for clique complexes corresponding to model and real networks with dimension $p = 0, 1, 2, 3$. In case of model networks, the statistics is reported for a particular instance of ER graph with $n = 1000$ and $p = 0.004$, WS graph with $n = 1000$, $k = 4$ and $p = 0.5$, BA graph with $n = 1000$ and $m = 2$, Spherical random graph produced from HGG model with $n = 1000$ and $\gamma = \infty$, and Hyperbolic random graph produced from HGG model with $n = 1000$ and $\gamma = 2$. Note that we omit self-loops in the real networks considered here.

Network	n_0	m_0	β_0	n_1	m_1	β_1	n_2	m_2	β_2	n_3	m_3	β_3
ER	1000	90	21	2007	1090	1021	7	0	0	0	0	0
WS	1000	123	1	2000	991	864	137	5	0	0	0	0
BA	1000	8	1	1996	949	942	55	0	0	0	0	0
Spherical	1000	172	126	2028	118	0	2029	180	0	1321	554	0
Hyperbolic	1000	144	144	2593	20	0	5440	426	0	11456	8159	0
US Power Grid	4941	573	1	6594	1671	1080	651	21	0	90	15	0
Email communication	1133	6	1	5451	1694	1186	5343	871	53	3419	1577	0
Route views	6474	17	1	12572	2459	2157	6584	627	19	5636	3335	0
Yeast protein interaction	1870	272	173	2203	424	318	222	12	0	41	12	0
Hamsterster frienship	1858	33	23	12534	4484	2970	16750	5324	1880	10015	4814	0
Euro road	1174	213	26	1417	425	237	32	1	0	0	0	0
Human protein interaction	3133	269	210	6149	2454	2298	1047	109	1	142	35	0

Application to model and real networks

Given a model or real network G , we limit our study of persistent homology to the 3-dimensional clique simplicial complex K corresponding to G . In other words, during the construction of the clique complex, we only include p -simplices which have dimension $0 \leq p \leq 3$ (See Theory section). Then using Algorithm 3 on this 3-dimensional clique complex K , we create the corresponding filtration based on the assigned weights to simplices using discrete Morse theory, and thereafter, make use of GUDHI [43], a C++ based library for Topological Data Analysis (<http://gudhi.gforge.inria.fr/>) to study the persistent homology of this filtration of K . Each hole of any dimension in K has a corresponding *birth* filtration weight and a *death* filtration weight (See Theory section). We normalize the *birth* and *death* filtration weights of all holes in K by dividing with $w_N = 1 + \max\{f(\alpha) \mid \alpha \in K\}$. In other words, w_N is 1 plus the maximum value among weights assigned to the simplices in K . We also make the convention that a normalized *death* filtration weight of 1 for a hole in K represents that the particular hole never *dies*.

A H_p -barcode diagram corresponding to a filtration of the clique complex K is a graphical representation containing horizontal line segments, each of which represents a p -hole in K , plotted against the x -axis ranging from 0 to 1 which corresponds to the normalized weights of simplices in K [44]. A horizontal line in the H_p -barcode diagram of K is referred to as a *barcode*. Thus, a barcode in the H_p -barcode diagram of K which begins at a x -axis value of w_1 and ends at a x -axis value of w_2 represents a p -hole in K whose *birth* and *death* weights are w_1 and w_2 , respectively. In figures 3, 4 and 5, we display the barcode diagrams for model and real-world networks analyzed here.

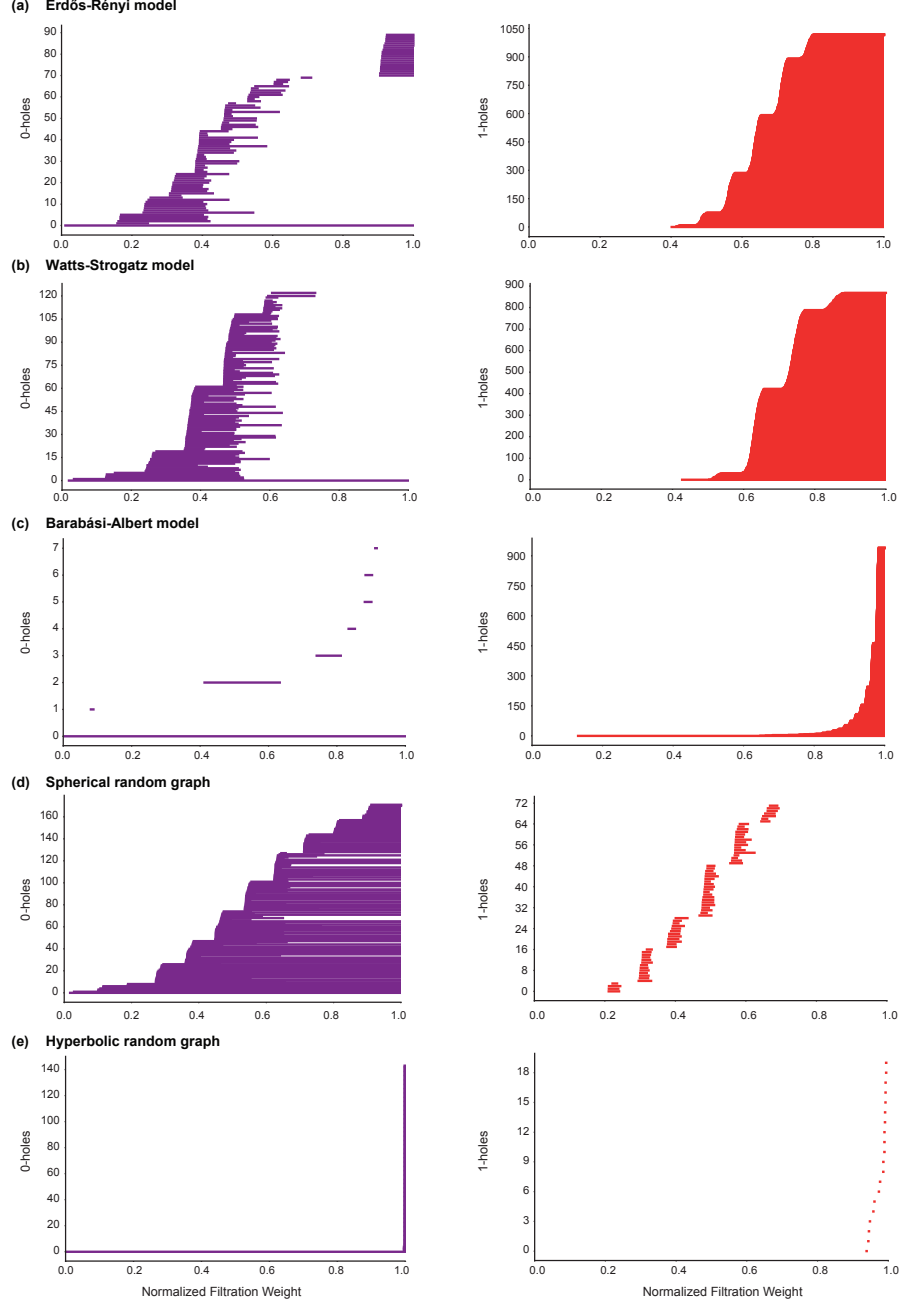


FIG. 3. Barcode diagrams for H_0 and H_1 in model networks. (a) ER model with $n = 1000$ and $p = 0.004$. (b) WS model with $n = 1000$, $k = 4$ and $p = 0.5$. (c) BA model with $n = 1000$ and $m = 2$. (d) Spherical random graphs produced from HGG model with $n = 1000$ and $\gamma = \infty$. (e) Hyperbolic random graphs produced from HGG model with $n = 1000$ and $\gamma = 2$.

Model Networks

In this work, we have investigated the persistent homology of unweighted and undirected graphs corresponding to five model networks, namely, ER, WS, BA, hyperbolic random graphs and spherical random graphs. The H_0 barcode diagram of BA networks indicate a low number of 0-holes in BA networks across the entire filtration (Figure 3). A standard result in algebraic topology [29] gives that the 0-Betti number of a simplicial complex K is equal to the number of connected components in K . In other words, the above observation indicates that the scale-free BA network has a strong tendency to maintain a low number of connected components during filtration (Figure 3).

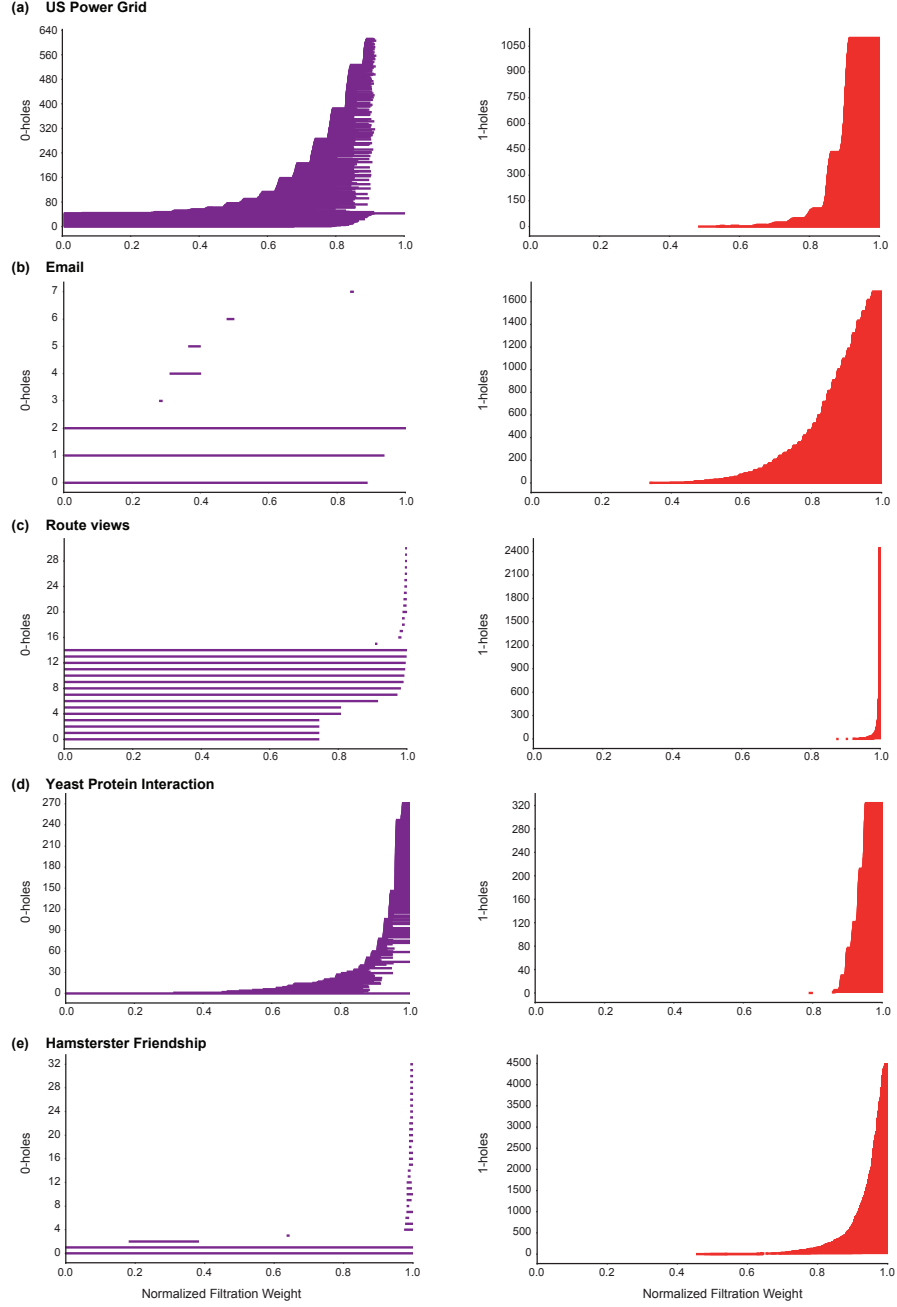


FIG. 4. Barcode diagrams for H_0 and H_1 in real networks. (a) US Power Grid. (b) Email communication. (c) Route views. (d) Yeast protein interaction. (e) Hamsterster friendship.

In contrast, both the random ER network and small-world WS network have a relatively high number of connected components at initial phase of the filtration and then progress towards a more connected network at later stages of the filtration (Figure 3). This indicates that the simplices in the clique complex which are key to the connectivity of the model networks are introduced very early into the filtration for the scale-free BA network while this is not the case for the random ER network or small-world WS network. The H_1 barcode diagram of BA networks also indicate late introduction of 1-holes during filtration in contrast to both ER and WS networks where 1-holes appear across a wider range of the filtration (Figure 3). Moreover, in ER and WS networks, it is interesting to observe that the 1-holes start to appear at roughly the same stage of filtration which corresponds to a sharp reduction in the number of connected components (Figure 3). In contrast to ER, WS and BA networks, the spherical and hyperbolic networks

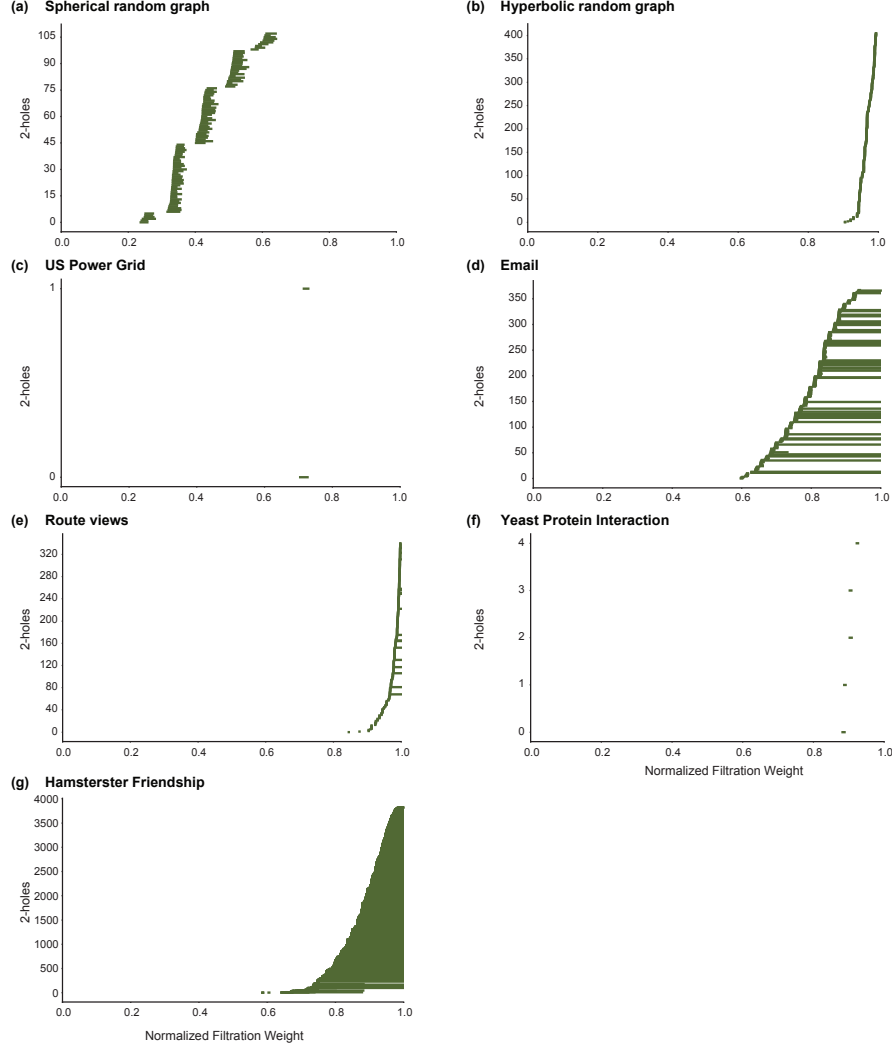


FIG. 5. Barcode diagrams for H_2 in model and real networks. (a) Spherical random graphs produced from HGG model with $n = 1000$ and $\gamma = \infty$. (b) Hyperbolic random graphs produced from HGG model with $n = 1000$ and $\gamma = 2$. (c) US Power Grid. (d) Email communication. (e) Route views. (f) Yeast protein interaction. (g) Hamsterster friendship.

are characterized by a relatively high 0-Betti number β_0 and a low 1-Betti number β_1 (Table I). Simply stated, this observation on the magnitude of β_0 indicates that both hyperbolic and spherical networks have a higher number of connected components in comparison to the ER, WS and BA networks of similar size, i.e., number of vertices, and average vertex degree (Table I). Although, both spherical and hyperbolic networks exhibit a higher number of connected components, they differ from each other with respect to the evolution of these connected components during filtration (Figure 3). The hyperbolic model maintains a relatively low number of connected components until very late in the filtration wherein there is a sharp increase in the number of connected components (Figure 3). This is in contrast with the behavior of the H_0 barcode diagram of the spherical model which exhibits a more distributed evolution of connected components during filtration (Figure 3). In addition, the low 1-Betti number, β_1 , for spherical and hyperbolic networks conveys the lack of 1-holes in these networks. A possible reason for this observation is the incidence of higher number of 2-simplices in the clique complex K of the spherical and hyperbolic networks in comparison to the ER, WS and BA networks (Table I). Note that the formation of a 2-simplex can potentially fill in a 1-hole, and thus, result in a low value for β_1 (See Theory section). Such a behaviour is also seen in the H_2 barcode diagrams of spherical and hyperbolic networks wherein the 2-holes have very short persistence since the addition of 3-simplices successively fill in the 2-holes (Figure 5). The H_2 barcode diagrams of ER, WS and BA networks do not provide any insight into network structure primarily due to a lack of higher-order correlations in these model networks that is essential for the formation of a 2-hole.

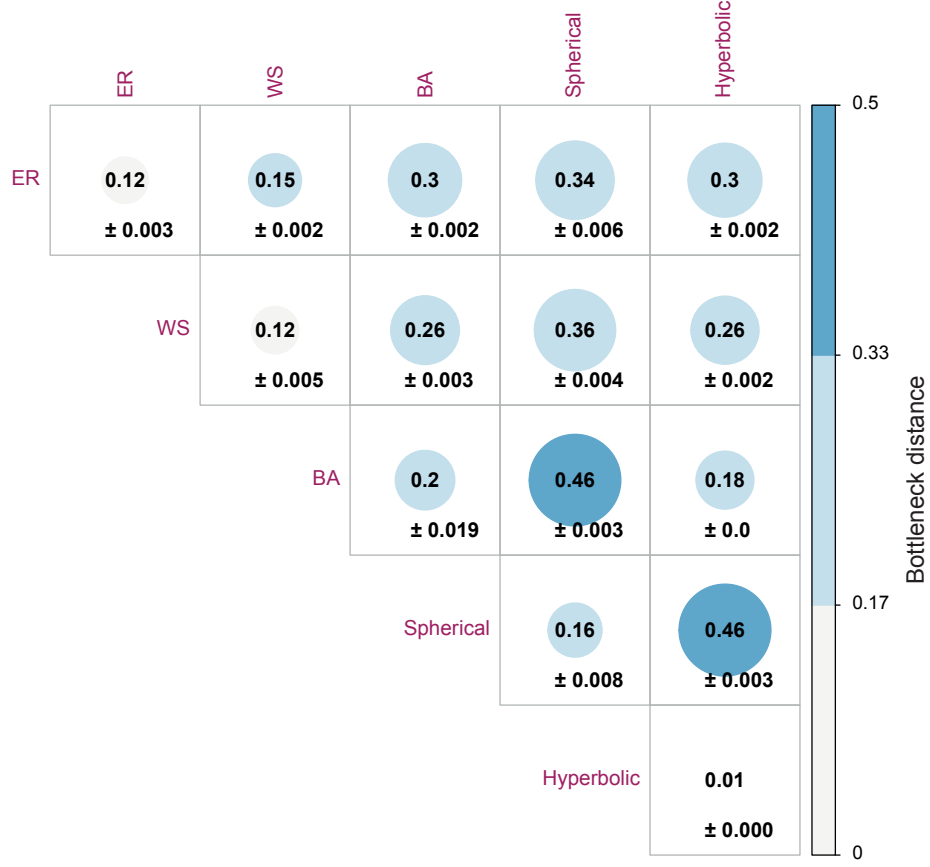


FIG. 6. Bottleneck distance between persistent diagrams of model networks, namely, ER model with $n = 1000$ and $p = 0.004$, WS model with $n = 1000$, $k = 4$ and $p = 0.5$, BA model with $n = 1000$ and $m = 2$, Spherical random graphs produced from HGG model with $n = 1000$ and $\gamma = \infty$, and Hyperbolic random graphs produced from HGG model with $n = 1000$ and $\gamma = 2$. For each of the five model networks, 10 random samples are generated by fixing the number of vertices n and other parameters of the model. We report the distance between two different models as the average of the distance between each of the possible pairs of the 10 sample networks corresponding to the two models along with the standard error.

A visual inspection of the barcode diagrams for the five model networks (Figure 3) suggests that the different models can be distinguished based on their persistent homology. In Theory section, we had introduced the bottleneck distance, 1-Wasserstein distance and 2-Wasserstein distance which can be employed to quantify the differences between persistence diagrams from filtration of clique complexes corresponding to different model networks. Recall that the persistence diagram of a d -dimensional simplicial complex K is a compact representation of the persistent homology of K which encompasses topological information across all d dimensions. Figure 6 gives the bottleneck distance between different model networks with the same size and average vertex degree. For each of the five model networks, 10 random samples are generated by fixing the number of vertices n and other parameters of the model. In figure 6, we report the distance between two different models as the average of the distance between each of the possible pairs of the 10 sample networks corresponding to the two models along with the standard error. We find a relatively higher distance between a random instance of a BA network and a random instance of a ER network with the same size and average degree (Figure 6). Similarly, we observe a relatively higher distance between a random instance of a BA network and a random instance of a WS network with the same size and average degree. In contrast, a relatively lower average distance is observed between a random instance of a ER network and a random instance of a WS network with the same size and average degree (Figure 6). These observations indicate a similarity between networks generated by ER and WS models in terms of their corresponding persistence diagrams and also show that the BA model exhibits topological properties that are different from the other two model networks of the same size and average degree. Moreover, the average distance between a random instance of a spherical network and a random instance of a hyperbolic network of the same size and average degree is very high (Figure 6). The last observation is a reflection of the differences in the persistent homology of the clique complexes corresponding to spherical and hyperbolic networks. Finally, the

qualitative nature of differences observed between persistence diagrams of different model networks using bottleneck distance as shown in figure 6 remain unchanged if the 1-Wassersstein or 2-Wasserstein distance is employed in place of the bottleneck distance (data not shown).

Table I lists the empirical data on the number of critical p -simplices, m_p , that our algorithm 1 achieves and the p -Betti number β_p of the clique complexes corresponding to the five model networks. In ER, WS and BA networks, we find that our algorithm achieves near-optimal results for m_p whose theoretical lower bound is given by β_p for $p = 0, 1, 2, 3$ (See Theory section). In contrast, in spherical and hyperbolic networks, our algorithm achieves near-optimal results for m_p in only dimensions $p = 0, 1, 2$ and the algorithm performs non-optimally for m_3 (Table I). We remark that the worst case scenario corresponds to all simplices in the clique complex being critical which is never attained by our algorithm in the analyzed networks.

Real networks

In this work, we have investigated the persistent homology of unweighted and undirected graphs corresponding to seven real-world networks and the barcode diagrams for these real networks is shown in figures 4 and 5. Based on the H_0 barcode diagrams, the behavior of most real networks considered here can be broadly classified into two categories. Real networks such as the Email communication, the Hamsterster friendship and the Route views exhibit a relatively low number of connected components across the entire range of filtration (Figure 4). On the other hand, the two biological networks, namely, the Yeast protein interaction and the Human protein interaction, exhibit a sharp increase in the number of connected components at the later stages of filtration. The H_0 barcode diagrams for the US Power Grid and Euro road do not conform with either of the above characterizations. The H_0 barcode diagram of the US Power Grid network reveals that though there exists only a single connected component at the end of the filtration, there are a considerable number of non-persisting connected components that appear and subsequently disappear during filtration (Figure 4). The H_0 barcode diagram of the Euro road network shows a more distributed increase in the number of connected components (data not shown). In the context of the H_1 barcode diagrams, the real networks considered here exhibit similar properties with 1-holes appearing late in the filtration (Figure 4). The H_2 barcode diagrams reveal a lack of 2-holes with long persistence in both biological networks, as well as the Route views network, the Euro road network and the US Power Grid network (Figure 5). In contrast, the social network, Hamsterster friendship, and the Email communication network exhibit a relatively high number of 2-holes with longer persistence (Figure 5). Table I also lists the empirical data on the number of critical p -simplices, m_p , that our algorithm 1 achieves and the p -Betti number β_p of the clique complexes corresponding to the seven real networks analyzed here. Like spherical and hyperbolic networks, our algorithm achieves near-optimal results for m_p in only dimensions $p = 0, 1, 2$ and the algorithm performs non-optimally for m_3 (Table I).

CONCLUSIONS

To conclude, we have proposed a systematic scheme based on discrete Morse theory to study the persistent homology of unweighted and undirected networks. Our methods leverage the concept of *critical* simplices to permit a reduced filtration scheme while simultaneously admitting a finer inspection of the changes in topology across the filtration of a clique complex corresponding to an unweighted network. Moreover, our proposed algorithm to construct a discrete Morse function on the clique complex of a simple graph achieves close to optimal number of critical simplices for several model and real networks that have been studied here, thereby reducing the length of the filtration sequence required to study the persistent homology. Furthermore, based on visual representations of persistent homology such as the barcode diagrams as well as quantitative information in the form of distance between persistence diagrams, our methods successfully distinguish various model networks that exhibit inherently different properties. This motivates the application of our methods to real-world networks. We report the results obtained for seven real-world networks that are well studied in the network science community and observe certain patterns in the evolution of their topological features across the filtration. For instance both biological networks, namely the Yeast protein interaction network and the Human protein interaction network exhibit similar characteristics with respect to the H_0 , H_1 and H_2 barcode diagrams. Similarly, both the Email network and the Hamsterster friendship network, exhibit shared features with respect to H_0 , H_1 and H_2 barcode diagrams that vary from the characteristics of the two biological networks considered here. Our observations hint at the ability and possible applications of our methods to detect and classify real-world networks that are inherently different.

Future directions and ongoing work include examining the significance of critical simplices in the context of real-world networks. In other words, we aim to determine whether a critical edge in the context of discrete Morse theory holds any key significance when it is viewed as a link between two real entities in a real-world network. We also intend

to explore the presence or absence of a correlation between the notion of critical simplices and network curvature. Since discrete Morse theory captures information about the Euler characteristic of the clique complex corresponding to a graph, the presence of such a correlation could potentially signify a close relationship between the discrete curvature of a graph and its topology, much like in the case of smooth, compact surfaces wherein the Gauss-Bonnet theorem relates the Gaussian curvature of a surface to its Euler characteristic.

ACKNOWLEDGMENTS

We thank Amritanshu Prasad for discussion. A.S. would like to acknowledge support from the Max Planck Society, Germany, through the award of a Max Planck Partner Group in Mathematical Biology, and I.R. from the Science and Engineering Research Board (SERB) of the Department of Science and Technology (DST) India through the award of a MATRICS grant [MTR/2017/000835].

-
- [1] G. Carlsson, Bulletin of the American Mathematical Society **46**, 255 (2009).
 - [2] P. Pranav, H. Edelsbrunner, R. Van de Weygaert, G. Vegter, M. Kerber, B. Jones, and M. Wintraecken, Monthly Notices of the Royal Astronomical Society **465**, 4281 (2016).
 - [3] D. Günther, J. Reininghaus, I. Hotz, and H. Wagner, in *2011 24th SIBGRAPI Conference on Graphics, Patterns and Images* (IEEE, 2011) pp. 25–32.
 - [4] M. Nicolau, A. Levine, and G. Carlsson, Proceedings of the National Academy of Sciences USA **108**, 7265 (2011).
 - [5] M. Morse, *The calculus of variations in the large*, Vol. 18 (American Mathematical Society, 1934).
 - [6] H. Edelsbrunner and J. Harer, Contemporary Mathematics **453**, 257 (2008).
 - [7] R. Forman, in *Geometry, Topology and Physics for Raoul Bott*, edited by S.-T. Yau (International Press of Boston, 1995).
 - [8] R. Forman, Séminaire Lothar. Combin. **48**, 1 (2002).
 - [9] D. J. Watts and S. H. Strogatz, Nature **393**, 440 (1998).
 - [10] A. L. Barabási and R. Albert, Science **286**, 509 (1999).
 - [11] R. Albert and A. L. Barabási, Reviews of Modern Physics **74**, 47 (2002).
 - [12] M. E. J. Newman, *Networks: An Introduction* (Oxford University Press, 2010).
 - [13] G. Bianconi, Europhysics Letters **111**, 56001 (2015).
 - [14] V. De Silva and R. Ghrist, Notices of the American mathematical society **54** (2007).
 - [15] D. Horak, S. Maletić, and M. Rajković, Journal of Statistical Mechanics: Theory and Experiment , P03034 (2009).
 - [16] G. Petri, M. Scombario, I. Donato, and F. Vaccarino, PLoS One **8**, e66506 (2013).
 - [17] G. Petri, P. Expert, F. Turkheimer, R. Carhart-Harris, D. Nutt, P. J. Hellyer, and F. Vaccarino, Journal of The Royal Society Interface **11**, 20140873 (2014).
 - [18] Z. Wu, G. Menichetti, C. Rahmede, and G. Bianconi, Scientific Reports **5**, 10073 (2015).
 - [19] A. Sizemore, C. Giusti, and D. Bassett, Journal of Complex Networks **5**, 245 (2016).
 - [20] O. Courtney and G. Bianconi, Physical Review E **95**, 062301 (2017).
 - [21] O. Courtney and G. Bianconi, Physical Review E **97**, 052303 (2018).
 - [22] H. Lee, H. Kang, M. Chung, B.-N. Kim, and D. Lee, IEEE transactions on medical imaging **31**, 2267 (2012).
 - [23] L. C. Freeman, Sociometry **40**, 35 (1977).
 - [24] M. Girvan and M. Newman, Proceedings of the National Academy of Sciences USA **99**, 7821 (2002).
 - [25] R. Sreejith, K. Mohanraj, J. Jost, E. Saucan, and A. Samal, Journal of Statistical Mechanics: Theory and Experiment , P063206 (2016).
 - [26] A. Samal, R. P. Sreejith, J. Gu, S. Liu, E. Saucan, and J. Jost, Scientific Reports **8**, 8650 (2018).
 - [27] B. Bollobas, *Modern Graph Theory* (Springer, 1998).
 - [28] A. Zomorodian and G. Carlsson, Discrete & Computational Geometry **33**, 249 (2005).
 - [29] J. Munkres, *Elements of algebraic topology* (CRC Press, 2018).
 - [30] D. Dummit and R. Foote, *Abstract algebra*, 3rd ed. (Wiley, 2003).
 - [31] D. Cohen-Steiner, H. Edelsbrunner, and J. Harer, Discrete & Computational Geometry **37**, 103 (2007).
 - [32] M. Kerber, D. Morozov, and A. Nigmatov, J. Exp. Algorithmics **22**, 1.4:1 (2017).
 - [33] P. Erdős and A. Rényi, Bull. Inst. Internat. Statist **38**, 343 (1961).
 - [34] D. Krioukov, F. Papadopoulos, M. Kitsak, A. Vahdat, and M. Boguná, Physical Review E **82**, 036106 (2010).
 - [35] R. Aldecoa, C. Orsini, and D. Krioukov, Computer Physics Communications **196**, 492 (2015).
 - [36] H. Jeong, S. P. Mason, A. L. Barabási, and Z. N. Oltvai, Nature **411**, 41 (2001).
 - [37] J. F. Rual, K. Venkatesan, T. Hao, T. Hirozane-Kishikawa, A. Dricot, N. Li, G. F. Berriz, F. D. Gibbons, M. Dreze, N. Ayivi-Guedehoussou, and *et al*, Nature **437**, 1173 (2005).
 - [38] J. Leskovec, J. Kleinberg, and C. Faloutsos, ACM Transactions on Knowledge Discovery from Data (TKDD) **1**, 2 (2007).
 - [39] L. Šubelj and M. Bajec, European Physical Journal B **81**, 353 (2011).
 - [40] R. Guimera, L. Danon, A. Diaz-Guilera, F. Giralt, and A. Arenas, Physical Review E **68**, 065103 (2003).

- [41] J. Kunegis, in *Proceedings of the 22nd International Conference on World Wide Web companion* (ACM, New York, NY, USA, 2013) pp. 1343–1350.
- [42] T. Lewiner, H. Lopes, and G. Tavares, *Experimental Mathematics* **12**, 271 (2003).
- [43] C. Maria, J.-D. Boissonnat, M. Glisse, and M. Yvinec, in *International Congress on Mathematical Software* (Springer, 2014) pp. 167–174.
- [44] R. Ghrist, *Bulletin of the American Mathematical Society* **45**, 61 (2008).